

NOVEL TESTS OF QUANTUM CHROMODYNAMICS IN ELECTRO-PRODUCTION*

Stanley J. Brodsky and Paul Hoyer**

Stanford Linear Accelerator Center, Stanford University, Stanford, California 94309

ABSTRACT

We discuss a number of ways in which single arm and coincident measurements of electroproduction on proton and nuclear targets can test fundamental QCD phenomena and provide constraints on hadronic wavefunctions. The topics include tests of color transparency, predictions for charm production at threshold, formation zone phenomena, and non-additive nuclear effects. We particularly emphasize the need for measurements which probe the short-range structure of hadronic and nuclear wave functions. In addition to the "extrinsic" gluonic and sea-quark contributions associated with radiation from single partons, perturbative QCD predicts an "intrinsic" hardness of the high-mass fluctuations of the wave function. These contributions can dominate heavy particle production at large x in the target fragmentation region and can be further enhanced in nuclear target reactions. Intrinsic hardness can also provide a possible explanation of the anomalous nuclear phenomena referred to as "cumulative production".

INTRODUCTION

A common goal of both particle and nuclear physics is to understand the structure of the nucleon and nucleus in terms of their fundamental quark and gluon degrees of freedom. The quark and gluon wavefunctions of hadrons play a role in virtually every aspect of high energy and electro-weak phenomenology. For example, detailed knowledge of these wavefunctions is crucial for the accurate calculations of weak decay amplitudes. The processes underlying strong and nuclear forces, color confinement, and jet hadronization in QCD all require an understanding of the coherent bound-state structure of hadrons.

The definitive probe of hadronic and nuclear structure is lepton scattering—not only the classic single-arm inclusive measurements of deep inelastic structure functions, but also coincidence lepto-production measurements of hadronic exclusive and semi-inclusive final states. The combination of elastic and inelastic lepton scattering is still the best "microscope" for probing the fundamental structure of the nucleon. Existing

* Work supported by the Department of Energy contract DE-AC03-76SF00515.

** Work supported by the Academy of Finland. Permanent address: Department of High Energy Physics, University of Helsinki, Finland

*Invited talk presented by S. J. Brodsky at the
Second European Workshop on Hadronic Physics with Electrons Beyond 10 GeV
Dourdan, France, October 8-12, 1990*

measurements at SLAC, Fermilab, and CERN have provided many constraints on the quark and gluon distributions that constitute the proton, but much remains unknown.

The focus of this talk will be on new opportunities for studying fundamental QCD phenomena in high energy electroproduction, particularly the opportunities made possible by a high-duty factor facility such as the PEGASYS experiment at SLAC, which proposes to make hermetic 4π measurements of the final state produced on polarized or unpolarized gas jet targets in the PEP e^\mp beams with $E_{lab} < 15 \text{ GeV}$, and a new high-intensity high-duty-factor electron machine in Europe which would access coincident electroproduction at higher energies. We will also mention some exciting physics opportunities which are possible using the unique high energy 50 GeV highly-polarized SLC beam at SLAC in single or double-arm deep inelastic lepton scattering experiments. The energy and momentum transfer range of all of these facilities are high enough such that the leading twist electron-quark scattering subprocess can dominate the cross section and that charm production near and above threshold can be studied.

At much higher energies, colliding electron-proton beams at HERA can test QCD evolution in the domain of very low x where gluon saturation and new types of higher twist contributions begin to dominate the structure functions.¹ Observing the fast fragments from the fast proton beam at HERA will permit another range of unique electroproduction experiments. For example, by detecting the forward proton in diffractive events $ep \rightarrow e'p'X$ one can study the QCD structure of the Pomeron (and the "Odderon"² in the case of exclusive channels where $X = \pi^0, \eta_0$, etc.). The production of high x_F particles and heavy quark systems in the proton fragmentation region even at low Q^2 can test QCD short-distance effects in the proton wavefunction.³

The traditional focus of electroproduction experiments has been the tests of the perturbative QCD predictions for the logarithmic evolution of the deep inelastic structure functions due to gluonic radiation from the struck quark. However, it has not been possible to completely test the QCD predictions for structure function evolution because of the persistent discrepancies between the present EMC, BCDMS, and SLAC measurements. A 50 GeV high precision experiment using the SLAC SLC beam would be ideal for removing these experimental conflicts. Just as important, at moderate values of momentum transfer there remain important questions and ambiguities concerning the magnitude and origin of higher twist corrections, the behavior of $R = \sigma_L/\sigma_T$, the origin of quark spin correlations, the shape of heavy quark structure functions, and the properties of the gluon distribution. Predictions for the Regge behavior of non-singlet structure functions have not been checked to high precision. In addition, recent lepton scattering experiments have claimed intriguing violations of QCD sum rules, anomalous spin correlations, unexpected charm particle effects, and significant non-additive nuclear corrections. These measurements all require confirmation and further investigation with a high energy, high intensity polarized beam such as the SLC 50 GeV beam at SLAC.

It is also important to extend measurements of the proton and neutron elastic and transition form factors to larger momentum transfer. These exclusive processes test QCD scaling laws and provide essential constraints on the "distribution amplitude" $\phi_N(x_1, x_2, x_3, Q)$ —the fundamental covariant wave function describing the correlations

of valence quarks in the nucleon bound-state.⁴

COINCIDENT ELECTROPRODUCTION EXPERIMENTS AT 50 GEV

One of the most important areas of QCD which has yet to be investigated in detail is the full structure of the final state in deep inelastic events, not just the photon fragmentation region, but also the target fragmentation region, where one can obtain constraints on the multi-particle components and heavy quark content of the nucleon wavefunction. There are many intriguing questions concerning jet evolution in electroproduction since the initial state begins with the production of a color triplet quark separating from a spectator system with the quantum numbers of a di-quark.

Nuclear targets can play a valuable role by filtering out certain components of the hadron wave function. In addition, the nuclear environment has the unique capability of probing and modifying the hadronization and dynamics of the recoil quark jet at the fermi scale. In a sense the nucleus plays a role analogous to Zeeman and Stark fields in atomic physics providing a practical way to modify the color field environment.

The following is a partial list of the types of coincidence electroproduction experiments which probe basic QCD phenomena. We will discuss several of these topics in more detail in the next sections. Further discussion and references are given in Ref. 5.

- *Formation zone physics*: study the quantum coherence and the time scales controlling the hadronization of quark jets propagating through a nucleus. The essential physics is controlled by the “target length condition”⁶ which states that there can be no change of state of an energetic system between two scattering centers separated by length L_A if the energy satisfies $E_{lab} > \Delta M^2 L_A$. Here ΔM^2 is the change of mass squared of the system, which is large if soft particles are emitted (small z , fixed k_{\perp}) and small if co-linear radiation is emitted.
- *Collision broadening*: study the final state elastic interactions of the recoil quark jet as it propagates through a nuclear target. The nuclear dependence of the transverse momentum of the recoil jet and its leading hadrons can give basic information on elastic quark-nucleon scattering. Some signs of this effect have been observed in low energy Drell-Yan reactions in nuclear targets. The target length condition does not eliminate such initial or final state interactions, although there may be a subtle effect due to the high virtuality of the scattered quark which could reduce the effective size of its elastic scattering cross section.
- *Shadowing and anti-shadowing*: study deviations from uniform nuclear linear A -dependence behavior in hard inclusive and exclusive scattering due to quark-nucleon interactions and long-range coherence. There has been recent progress in relating shadowing and anti-shadowing to the Pomeron and Reggeon exchange contributions in the quark-nucleon scattering amplitude.⁷
- *Color Transparency and Color Filter*: study the nuclear dependence of general quasi-elastic reactions to separate short-range perturbative versus long-range non-perturbative phenomena. As mentioned above there are many possible tests of color transparency in nuclei including exclusive pion and kaon production processes, diffractive vector meson production, and also charmonium production.

- *Jet Fragmentation Studies:* Confirm QCD predictions for jet fragmentation at the leading and next-to-leading twist level; test predictions⁸ for dominant $1/Q^2$ contributions to jet fragmentation at $z \sim 1$. The recent extended factorization theorem of Sterman and Qiu⁹ makes it imperative that one search for these higher twist longitudinal current contributions since they are directly connected to contributions seen in large x meson induced Drell-Yan reactions.
- *Intrinsic Charm:* confirm the anomalous components of the charm structure functions of the proton seen at large x_{Bj} . Study charmonium and open charm production in the target fragmentation region. We will discuss this important physics in more detail in the following section.
- *Photo- and electroproduction of charmonium states:* provide constraints on the gluon distribution of the proton in the photon-gluon fusion model; use the nuclear dependence to find non-additive gluon effects and determine $\sigma_{\psi N}$.
- *Nuclear-bound quarkonium:* study electroproduction just below the threshold in $\gamma^* A \rightarrow \eta_c A$ reactions to identify nuclear-bound charmonium states such as $\eta_c - {}^3\text{He}$, novel bound states formed by the attractive QCD van der Waals gluonic exchange potential.
- *Intrinsic Hardness:* test PQCD predictions for high transverse momentum pair correlations in proton and nuclear intrinsic momentum wave functions.
- *Cumulative Effect in $\gamma^* A \rightarrow HX$:* measure the production of fast hadrons in the backward direction well beyond the kinematic limit for a proton target; identify anomalous short-range correlations predicted by PQCD.
- *Quark-diquark structure of the proton:* study correlations of final state hadrons in the target fragmentation region.
- *Prompt photon emission:* study anomalous soft-photon production as a clue to hadronization mechanisms and final state quark scattering.
- *Diffraction electroproduction such as $\gamma^* p \rightarrow \rho p$ and $\gamma^* p \rightarrow J/\psi p$ on proton or nuclear targets:* probe Pomeron coupling to systems of variable size and measure multi-gluon exchange form factors.
- *Diffraction π and η photoproduction:* identify and probe the QCD “Odderon” –odd C contribution to high energy scattering from three gluon exchange, etc.
- *Exclusive channels, such as $ep \rightarrow eN^*$ at large Q^2 :* measure the fundamental distribution amplitudes of the proton and baryonic resonances; extend meson form factor measurements; test PQCD scaling laws for $\gamma^* p \rightarrow MN$ reactions.
- *Exclusive nuclear amplitudes such as $\gamma^* d \rightarrow np$:* test PQCD “reduced amplitude” predictions.
- *Virtual Compton scattering at high momentum transfer $\gamma^* p \rightarrow \gamma p$:* check perturbative QCD predictions.
- *Compton scattering on nuclei such as $\gamma^* D \rightarrow \gamma D$:* search for “hidden color” multi-quark resonances predicted by QCD which could dominate the large angle reaction.

- *Electron-positron asymmetry in $e^\pm p \rightarrow e^\pm \gamma X$* : measure fractional charges of quarks and a new type of valence structure function.
- *Spin-one structure functions for electroproduction on a deuteron target*: test PQCD predictions for high spin structure functions¹⁰ requiring multi-quark coherence.
- *Anomalous spin correlations*: study the spin structure functions and helicity effects in the final state, including spin correlations of strange hadrons.

COLOR TRANSPARENCY

One of the most interesting QCD phenomena that can be tested in electroproduction is “color transparency.”¹¹ The basic measurement requires the observation of quasi-elastic nearly-coplanar electron-proton scattering in a nuclear target without extra hadronic production. A basic feature of perturbative QCD is the assertion that a hadron can only scatter through large momentum transfer and stay intact if its wavefunction is in a fluctuation⁴ which contains only valence quarks at small transverse separation $b_\perp \sim 1/Q$. QCD then makes the remarkable prediction that the cross section for large momentum transfer quasi-elastic scattering such as $ep \rightarrow ep$ in a nucleus will be unaffected by final-state absorption corrections, since the scattering is dominated by a configuration of the valence-quark wavefunction of the proton which has a small color dipole moment. (By definition, quasi-elastic processes are nearly coplanar, integrated over the Fermi motion of the protons in the nucleus. Such processes are nearly exclusive in the sense that no extra hadrons are allowed in the final state.) Thus, at large momentum transfer and energies, quasi-elastic exclusive reactions are predicted to occur uniformly in the nuclear volume, unaffected by initial or final state multiple-scattering or absorption of the interacting hadrons. This remarkable phenomenon is called color transparency reflecting the transparency of the nucleus to small color-singlet configurations.

There are many tests of color transparency in electroproduction in addition to quasi-elastic ep scattering, such as baryon resonance production, $\gamma^* p \rightarrow \pi^+ n, \gamma^* n \rightarrow K^- p, \gamma^* p \rightarrow \rho p$ at high transverse momentum or at high photon mass. In each case one can test for the dominance of hard-scattering dominance of the exclusive reaction. The ability to isolate photoproduction on neutrons provides further checks on QCD predictions for the underlying subprocesses. In the case of high energy J/ψ photoproduction, the initially formed $c\bar{c}$ can propagate freely through the nucleus as a small color-singlet forming the charmonium state outside of the nucleus.¹¹ As emphasized by Pire and Ralston,¹² the nucleus filters out the non-perturbative soft-contributions.

There are two conditions which set the kinematic scale where PQCD color transparency should be evident and quasi-elastic scattering cross section will be additive in proton number in the nuclear target. First, the hard scattering subprocess must occur at a sufficiently large momentum transfer so that only small transverse size wavefunction components $\psi(x_i, b_\perp \sim 1/Q)$ with small color dipole moments dominate the reaction. Second, the state must remain small during its transit through the nucleus. The expansion distance is controlled by the time in which the small Fock component mixes with other Fock components. By Lorentz invariance, the time scale $\tau = 2E_{\bar{p}}/\Delta M^2$

grows linearly with the energy of the hadron in the nuclear rest frame, where $\Delta\mathcal{M}^2$ is the difference of invariant mass squared of the Fock components. The scale in momentum transfer that sets the onset of color transparency reflects the coherent formation time of the nucleon system. An elegant quantum mechanical treatment of this aspect of the color transparency phenomenon is given in Refs. 12, 13, and 14. The first test of this phenomenon in electroproduction will be the NE-18 $eA \rightarrow ep$ ($A - 1$) two-arm coincidence test using the 9 GeV NPAS injector at SLAC.

More generally, it is possible to use a nucleus as a “color filter”^{15,12} to separate and identify the threshold and perturbative contributions to the scattering amplitude. If the interactions of an incident hadron are controlled by gluon exchange, then the nucleus will be transparent to those fluctuations of the incident hadron wavefunction which have small transverse size. Such Fock components have a small color dipole moment and thus will interact weakly in the nucleus; conversely, Fock components with slow-moving massive quarks cannot remain compact. They will interact strongly and be absorbed during their passage through the nucleus.

The only existing test of color transparency is the measurement of quasi-elastic large angle pp scattering in nuclei at Brookhaven.¹⁶ The transparency ratio is observed to increase as the momentum transfer increases, in agreement with the color transparency prediction. However, in contradiction to perturbative QCD expectations, the data suggests, surprisingly, that normal Glauber absorption seems to recur at the highest energies of the experiment $p_{\text{lab}} \sim 12 \text{ GeV}/c$. Even more striking is that this is the same energy at which the spin correlation A_{NN} is observed to rise dramatically:¹⁷ the cross section for protons scattering with their spins parallel and normal to the scattering plane is found to be four times as big as the cross section for anti-parallel scattering, which is again in strong contradiction to PQCD expectations.

It is important to note¹⁸ that the breakdown of color transparency and the onset of strong spin-spin correlations both occur at $\sqrt{s} \sim 5 \text{ GeV}$ or $p_{\text{lab}} \sim 12 \text{ GeV}/c$, which is the charm threshold occurs in pp collisions. At this energy the charm quarks are produced at rest in the center of mass, and all of the eight quarks have zero relative velocity. The eight-quark cluster thus moves through the nuclear volume with just the center-of-mass velocity. Even though the initial cluster size is small (since all valence quarks had to be at short transverse distances to exchange their momenta), the multi-quark nature and slow speed of the cluster implies that it will expand rapidly and be strongly absorbed in the nucleus. This Fock component will then not contribute to the large-angle quasi-elastic pp scattering in the nucleus: It will be filtered out.

The charm threshold effect will couple most strongly to the $J = L = S = 1$ partial wave in pp scattering.¹⁸ (The orbital angular momentum of the pp state must be odd since the charm and anti-charm quarks have opposite parity.) This partial wave predicts maximal spin correlation in A_{NN} . Thus, if this threshold contribution to the $pp \rightarrow pp$ amplitude dominates the valence quark QCD amplitude, one can understand both the large spin correlation and the breakdown of color transparency at energies close to charm threshold. Thus the nucleus acts as a filter, absorbing the threshold contribution to elastic pp scattering, while allowing the hard scattering perturbative QCD

processes to occur additively throughout the nuclear volume.¹² Experimentally, a strong enhancement of A_{NN} is observed at the threshold for strange particle production, which is again consistent with the dominance of the $J = L = S = 1$ partial wave helicity amplitude. The large size of A_{NN} observed at both the charm and strange thresholds is striking evidence of a strong effect on elastic amplitudes due to threshold production of fermion-antifermion pairs.

If the above explanation of the A_{NN} and color transparency anomalies is correct then one can identify the effect of heavy quark thresholds in hadron collisions by studying their elastic scattering at large angles. Through unitarity, even a threshold cross section of only $1 \mu b$ for the production of open charm in pp collisions will have a profound influence on the $pp \rightarrow pp$ scattering at $\sqrt{s} \sim 5 \text{ GeV}$, because of its very small cross section at 90° . The production of charm at threshold implies that there is a contribution with massive, slow-moving constituents to the pp elastic amplitude which can modify the ordinary PQCD predictions, including dimensional counting scaling laws, helicity dependence, angular dependence, and especially the "color transparency" of quasi-elastic pp scattering in a nuclear target. Note that this effect would not affect the onset of color transparency in quasi-elastic ep scattering, but it could appear in other color transparency tests in electroproduction such as $eA \rightarrow e'\pi n(A-1)$.

PHOTOPRODUCTION AND ELECTROPRODUCTION OF NUCLEAR BOUND QUARKONIUM

In general one expects that heavy quark systems produced near threshold will experience strong final state interactions since there is a long time for the system to interact strongly. Thus one expects enhancements to open charm and charmonium in electroproduction at threshold beyond that expected from photon-gluon fusion from both initial state intrinsic charm components in the wavefunction (see the next section) and multi-gluon exchange contributions. The situation could be even more interesting in a nuclear target.

For example, consider the reaction $\gamma {}^3\text{He} \rightarrow {}^3\text{He}(c\bar{c})$ where the charmonium state is produced nearly at rest. At the threshold for charm production, the produced particles will be slow (in the center of mass frame) and will fuse into a compound nucleus because of the strong attractive nuclear force. The charmonium state will be attracted to the nucleus by the QCD gluonic van der Waals force. One thus expects strong final state interactions near threshold. In fact, it is argued in Ref. 19 that the $c\bar{c}$ system could bind to the ${}^3\text{He}$ nucleus. It is thus possible that a new type of exotic nuclear bound state will be formed: charmonium bound to nuclear matter. Such a state should be observable at a distinct $\gamma {}^3\text{He}$ center of mass energy, spread by the width of the charmonium state, and it will decay to unique signatures. The binding energy in the nucleus gives a measure of the charmonium's interactions with ordinary hadrons and nuclei; its hadronic decays will measure hadron-nucleus interactions and test color transparency starting from a unique initial state condition.

In QCD, the nuclear forces are identified with the residual strong color interactions due to quark interchange and multiple-gluon exchange. Because of the identity of the quark constituents of nucleons, a short-range repulsive component is also present (Pauli-blocking). From this perspective, the study of heavy quarkonium interactions in nuclear

matter is particularly interesting: due to the distinct flavors of the quarks involved in the quarkonium–nucleon interaction there is no quark exchange to first order in elastic processes, and thus no one–meson–exchange potential from which to build a standard nuclear potential. For the same reason, there is no Pauli–blocking and consequently no short–range nuclear repulsion. The nuclear interaction in this case is purely gluonic and thus of a different nature from the usual nuclear forces.

The production of nuclear–bound quarkonium would be the first realization of hadronic nuclei with exotic components bound by a purely gluonic potential. Furthermore, the charmonium–nucleon interaction would provide the dynamical basis for understanding the spin–spin correlation anomaly in high energy pp elastic scattering.¹⁸ In this case, the interaction is not strong enough to produce a bound state, but it can provide an enhancement at the heavy–quark threshold characteristic of an almost–bound system.²⁰

THE HEAVY QUARK CONTENT OF NUCLEONS

One of the most intriguing unknowns in nucleon structure is the strange and charm quark structure of the nucleon wavefunction. The EMC spin crisis measurements indicate a significant $s\bar{s}$ content of the proton, with the strange quark spin strongly anti-correlated with the proton spin. Just as striking, the EMC measurements of the charm structure function of the proton at large x_B ; ~ 0.4 appear to be considerably larger than that predicted by the conventional photon-gluon fusion model, indicating an anomalous charm content at large values of x .²¹ The probability of intrinsic charm has been estimated²¹ at 0.3%.

In the following sections we discuss the QCD physics of hadronic wavefunctions and the basis for understanding intrinsic heavy quark states and other high mass components of the hadronic and nuclear wavefunctions. Coincidence measurements of strange and charmed particles in high energy electroproduction to test these anomalies are important and challenging experiments. One of the most interesting areas of investigation are the exclusive charm channels, *e.g.*, $\gamma^*p \rightarrow \bar{D}\Lambda_c$, to test predictions of possibly enhanced cross sections near threshold. Such measurements of constrained charmed meson and charmed baryon final states could provide a definitive measurements of charmed baryon decay branching ratios. One of the major uncertainties in the present determinations of the charmed baryon production cross sections in hadron collisions is the large uncertainty in the branching fractions for the Λ_c .

Complete measurements of the heavy quark content of protons and nuclei will require a high energy high duty factor electron facility, such as the European facility discussed at this meeting. Initially, the PEGASYS facility at SLAC together with a 4π detector such as the Mark II or TPC, would provide an ideal laboratory for large acceptance coincidence electroproduction experiments on polarized or unpolarized gas jet targets, including studies of charm production near and above threshold. In addition the 9 GeV electron ring which could be available at a high intensity asymmetric B–factory would permit higher luminosity coincident electroproduction measurements. A PEGASYS-type facility at a B–factory could provide a sensitive probe of fundamental

baryon structure as well as being a potential factory for highly constrained charmed baryons.

PROBING THE FOCK STATE STRUCTURE OF HADRONS

One of the most useful concepts in QCD hadronic physics is the Fock state expansion of the hadron wavefunction in terms of its quark and gluon constituents.^{22,4} The physical content of a hadron can be represented by its light-cone wavefunctions $\psi_n(x_i, p_{\perp i}, \lambda_i)$, the projection of the hadron wavefunction on the set of complete Fock states defined at fixed light-cone time $\tau = t + z/c$. Here $x_i = (E_i + p_{L i})/(E + p_L)$, with $\sum_i x_i = 1$, is the fractional (light-cone) momentum carried by parton i . The lowest Fock state of the proton is the color singlet three quark valence state ψ_3 . Given these wavefunctions, one can compute many physical properties of hadrons. For example, electroweak form factors, magnetic moments, etc. are given simply by the overlap integral of initial and final state wavefunctions, summed over all n . The quark and gluon structure functions are the probability distributions obtained by summing and integrating over the squares of the light-cone wavefunctions. Weak decay and operator product matrix elements are given in terms of projections of the ψ_n . Exclusive reactions at large momentum transfer are computed from the overlap of the hard-scattering quark-gluon scattering amplitude T_H convoluted with the hadron distribution amplitudes $\phi(x_i; Q)$. The distribution amplitude is the fundamental probability amplitude describing the longitudinal momentum fractions of the valence quarks; it is defined by integrating the valence wavefunction over transverse momentum $p_{\perp i}$ up to the momentum transfer scale Q .

The determination of the light-cone wavefunctions requires diagonalizing the light-cone Hamiltonian on the free Fock basis. This in fact has been done for QCD in one-space and one time dimension using a momentum space method of discretization called discretized light-cone quantization (DLCQ).²³ Efforts are now proceeding to solve the much more complex problem in 3+1 dimensions. Even without explicit solutions, a great deal of information can be obtained at high k_{\perp} or the end-point $x \sim 1$ region using perturbative QCD since the quark and gluon propagators become far off-shell. In particular one can obtain dimensional and spectator counting rules which determine the end-point behavior of structure functions, etc.

It is useful to distinguish *extrinsic* and *intrinsic* contributions to structure functions. The extrinsic contributions are associated with the substructure of a single quark and gluon of the hadron. Such contributions lead to the logarithmic evolution of the structure functions and depend on the momentum transfer scale of the probe. The intrinsic contributions involve at least two constituents and are associated with the bound state dynamics independent of the probe. The intrinsic gluon distributions are closely related to the retarded mass-dependent part of the bound-state potential of the valence quarks. A rather complete model for the intrinsic gluon distribution of the proton including helicity correlations that satisfies known constraints is given in Ref. 24.

It is also important to distinguish extrinsic and intrinsic contributions to the sea quark distributions. For example, the extrinsic contributions to the charm quark sea only depends logarithmically on the charm quark mass at $Q^2 \gg m_c^2$. The intrinsic con-

tributions are suppressed by two or more inverse powers of the heavy quark mass. Nevertheless, these contributions can still be important and dominate in certain kinematic regions, particularly large x . The intrinsic contributions have a number of remarkable properties which we return to below.

It is particularly convenient to use the Fock expansion to describe the interactions of a hadron moving at large momentum P (although the results are frame independent when light-cone quantization is used.) For example, to describe ep scattering in the CM or HERA colliding beam configuration we consider the Fock expansion of the proton in QCD,

$$|p\rangle = |uud\rangle + |uudg\rangle + \dots + |uudQ\bar{Q}\rangle + \dots \quad (1)$$

where $q(Q)$ refers to a light (heavy) quark and g to a gluon. At high energies, most scattering processes in electroproduction only involve states of the proton that were formed long before the collision takes place. The individual Fock components in (1) have "lifetimes" Δt (before mixing with other components) which can be estimated from the uncertainty relation $\Delta E \Delta t \sim 1$. At large hadron energies E the energy difference becomes small,

$$\Delta E \approx \frac{1}{2E} \left(m^2 - \sum_i \frac{m_i^2 + p_{Ti}^2}{x_i} \right). \quad (2)$$

Fock components for which $1/\Delta E$ is larger than the interaction time have thus formed before the scattering and can be regarded as independent constituents of the incoming wave function. At high energies only collisions with momentum transfers commensurate with the center of mass energy, such as deep inelastic lepton scattering ($Q^2 \sim 2m\nu$) and jet production with $p_T \sim \mathcal{O}(E_{cm})$ produce states with lifetimes as short as the scattering time.

The above arguments show that a typical scattering process is essentially determined by the mixture of incoming Fock states, *i.e.*, by the wave functions of the scattering particles. This is true even for collisions with very heavy quarks or with particles having very large p_T in the final state, provided only that the momentum transferred in the collision is small compared to E_{cm} . The cross sections for such collisions are thus determined by the probability of finding the corresponding Fock states in the beam or target particle wave functions; *cf.* Eq. (1). An example of this is provided by the Bethe-Heitler process of e^+e^- pair production in QED. A high energy photon can materialize in the Coulomb field of a nucleus into an e^+e^- pair through the exchange of a very soft photon. The creation of the massive e^+e^- pair occurs long before the collision and is associated with the wave function of the photon. The collision process itself is soft and does not significantly change the momentum distribution of the pair. Similarly, heavy quark production in hadron collisions or electroproduction at any Q^2 at high energies ($E_{cm} \gg m_Q$) is governed by the hard (far off energy-shell) components of the hadronic wave functions.³

THE STRUCTURE OF INTRINSICALLY HARD STATES

The leading extrinsic contribution to heavy quarks in a hadronic wave function is one gluon splitting into a heavy quark pair, $G \rightarrow Q\bar{Q}$ (Fig. 1a). We call this contribution extrinsic since it is independent of the hadron wave function, except for its gluon content. The extrinsic heavy quarks are, in a sense, "constituents of the gluon". The extrinsic heavy quark wave function has the form

$$\Psi^{extrinsic}(q\bar{q}Q\bar{Q}) = \Gamma_G T_H(G \rightarrow Q\bar{Q}) \frac{1}{E\Delta E} \quad (3)$$

The square of the gluon amplitude Γ_G gives the ordinary gluon structure function of the hadron. The gluon splitting amplitude T_H is of order $\sqrt{\alpha_s(m_Q^2 + p_{TQ}^2)}$, and ΔE is the energy difference (2). The integral of the extrinsic probability $|\Psi^{extrinsic}|^2$ over p_{TQ}^2 for $p_{TQ} \lesssim \mathcal{O}(m_Q)$ brings a factor of m_Q^2 . Hence we see that the probability of finding extrinsic heavy quarks (or large p_T) in a hadronic wave function is actually independent of the quark mass (or p_T). This is related to the quadratic divergence of the quark loop in Fig. 1b. The production cross section of the $Q\bar{Q}$ pair is still damped by a factor $1/m_Q^2$, this being the approximate transverse area of the pair.

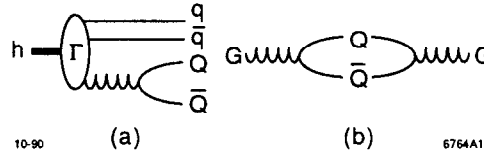


Figure 1. (a) Gluon splitting gives rise to extrinsic heavy quarks in a hadron wave function. The pointlike coupling to the gluon implies that all quark masses and all transverse momenta are generated with equal probability. (b) In the squared amplitude, this is seen as a quadratic divergence of the quark loop.

Intrinsic heavy quark Fock states²⁵ arise from the spatial overlap of light partons. Typical diagrams are shown in Fig. 2. The transverse distance between the participating light partons must be $\lesssim \mathcal{O}(1/m_Q)$ for them to be able to produce the heavy quarks. The wave function of the intrinsic Fock state has the general structure

$$\Psi^{intrinsic}(q\bar{q}Q\bar{Q}) = \Gamma_{ij} T_H(ij \rightarrow Q\bar{Q}) \frac{1}{E\Delta E} \quad (4)$$

Here Γ_{ij} is the two-parton wave function, which has a dimension given by the inverse hadron radius. $T_H(ij \rightarrow Q\bar{Q})$ is the amplitude for two (or, more generally, several) light partons i, j to create the heavy quarks, and ΔE is the energy difference (2) between the heavy quark Fock state and the hadron. A sum over different processes, and over

the momenta of the light partons, is implied in (4). In renormalizable theories such as QCD, the amplitude T_H is dimensionless. Hence, up to logarithms, the probability $|\Psi^{intrinsic}|^2$ for intrinsic heavy quarks is of $\mathcal{O}(1/m_Q^2)$ (after the p_T^2 integration). This is smaller by $1/m_Q^2$ as compared to the probability (3) for extrinsic heavy quarks,^{25,26} as is true of higher twist. The relative suppression is due to the requirement that the two light partons be at a distance $\lesssim 1/m_Q$ of each other in the intrinsic contribution.

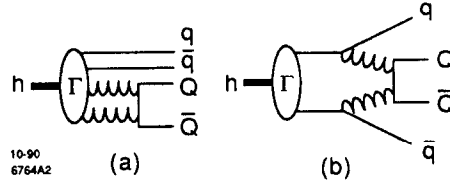


Figure 2. Intrinsic heavy quark contributions to a hadronic wave function, generated by (a) gluon fusion and (b) light quark scattering. The large mass of the produced quark implies that the participating light partons must be at a small transverse separation.

In contrast to the extrinsic contribution (3), which depends only on the inclusive single gluon distribution, an evaluation of the intrinsic Fock state (4) requires a knowledge of multiparton distributions amplitudes. In particular, we need also the distribution in transverse distance between the partons. Our relative ignorance of the multiparton amplitudes Γ_{ij} for hadrons makes it difficult to reliably calculate the magnitude of the intrinsic heavy quark probability. We can, however, estimate²⁵ the distribution of intrinsic quarks from the size of the energy denominator ΔE , as given by (2). It is clear that those Fock states which minimize ΔE , and hence have the longest lifetimes, also have the largest probabilities. In fact, taking

$$|\Psi^{intrinsic}|^2 \sim 1/(\Delta E)^2, \quad (5)$$

one finds that the maximum is reached for

$$x_i = \frac{\sqrt{m_i^2 + p_{Ti}^2}}{\sum_i \sqrt{m_i^2 + p_{Ti}^2}}, \quad (6)$$

implying equal (longitudinal) velocities for all partons. The rule (5) has been found to successfully describe the hadronization of heavy quarks.^{27,28}

Using the probability (5), we see from (6) that partons with the largest mass or transverse momentum carry most of the longitudinal momentum. This has long been one of the hallmarks of intrinsic charm. We also note that the intrinsic heavy quark states have a larger transverse size than the extrinsic ones, although both tend to be

small, of $\mathcal{O}(1/m_Q^2)$. The extrinsic heavy quarks are produced by a single (pointlike) gluon (Fig. 1), whereas the intrinsic mechanism is more peripheral (Fig. 2). This means that rescattering and absorption effects for intrinsic states produced on heavy nuclei will be relatively more significant, compared to that for extrinsic states. In addition to the heavy quarks Q , such rescattering may affect the light partons involved in the intrinsic state (*e.g.*, the quarks q in Fig. 2(b)). These light quarks tend to be separated by a larger transverse distance than the heavy quarks, further enhancing the rescattering.

Consider now the formation of intrinsic heavy quark states in nuclear wave functions. At high energies, partons from different nucleons can overlap, provided only that their transverse separation is small. Thus the partons which create intrinsic heavy quarks in Fig. 2 can come from two nucleons which are separated by a longitudinal distance in the nucleus. Now it is reasonable to assume that partons belonging to different nucleons are uncorrelated, *i.e.*, that the two-parton amplitude Γ_{ij} in Eq. (4) is proportional to the product $\Gamma_i \Gamma_j$ of single parton amplitudes. Hence the amount of intrinsic charm in nuclei may possibly be more reliably calculated than for hadrons. The probability for intrinsic charm will increase with the nuclear path length as $A^{1/3}$. Moreover, the total longitudinal momentum of the intrinsic quark pair, being supplied by two different nucleons, can be larger than in a single hadron, and can in fact exceed the total momentum carried by one nucleon.

All that we have said above concerning heavy quark Fock states applies equally to states with light partons carrying large transverse momentum. Extrinsic and intrinsic mechanisms for generating large p_T in hadronic wave functions are shown in Fig. 3. Using Eq. (5) as a guideline for the probability of intrinsic hardness, we see in fact that the parton mass and p_T appear in an equivalent way. Remarkably QCD predicts that these high mass fluctuations occur in the nucleon and nuclear wavefunctions with the minimal power law fall off: $P(\mathcal{M}^2 > \mathcal{M}_0^2) \sim 1/\mathcal{M}_0^2$. We again expect that the intrinsic mechanism will be dominant at large x_F , and in particular in the cumulative ($x_F > 1$) region of nuclear wave functions. In each case one can materialize the large mass fluctuations in electroproduction even at minimal photon mass Q^2 . The crucial experimental requirement is the ability to identify the target fragments in the target fragmentation region.

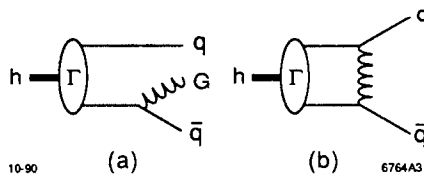


Figure 3. (a) An extrinsic contribution to large transverse momentum partons in a hadron and (b) an intrinsic contribution.

The possibility of parton fusion has been considered previously in the context of the evolution of parton distributions with momentum transfer (Q^2).^{29,30} At very large Q^2 and small x , the number of gluons can become large enough to force them to overlap and

coalesce. Our emphasis here is different. We are interested in rare phenomena at large x , where processes involving two or more gluons and valence quarks can give dominant effects, even though the likelihood for such fluctuations is small. The colliding partons in Figs. 1-3 are to be thought of (in a first approximation) as nearly on-shell, and having small p_T . Only the part of the processes in Fig. 3 leading to large p_T partons is to be considered as a new contribution to the wave function. In particular, the fusion of two partons into one (e.g., $qG \rightarrow q$), which cannot give large p_T , is a part of the non-perturbative wave functions Γ , and hence does not contribute to intrinsic hardness.

CHARM PRODUCTION IN HADRON AND NUCLEAR COLLISIONS

The concept of intrinsic charm was originally inspired by hadron-hadron scattering experiments³¹ showing unexpectedly abundant charm production at large $x_F = 2p_{charm}/E_{cm}$. When extrapolated to small x_F , the data suggested total charm cross sections in the millibarn range, far beyond the predictions (20 - 50 μb) of the standard QCD gluon fusion process (cf. Fig. 4(a)). Later data with good acceptance at low x_F showed that the total charm cross section actually is compatible with the gluon fusion process.³² Nevertheless, more evidence was also obtained showing that charm production at large x_F , albeit a small fraction of the total cross section, still is larger than expected.³³ The large x_F data also shows correlations (leading particle effects) with the quantum numbers of the beam hadron that are incompatible with gluon fusion.³⁴

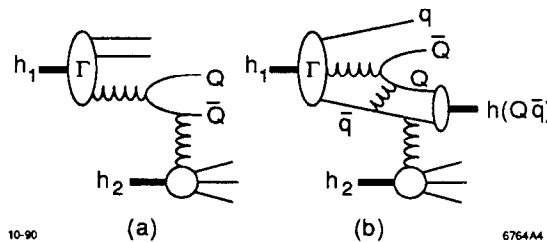


Figure 4. (a) The gluon-gluon fusion process in QCD. At high energies, the extrinsic $Q\bar{Q}$ pair preforms in the incoming wave function and is put on mass-shell by a soft gluon from the target. (b) An example of intrinsic heavy quark production. The heavy quark can get additional momentum from a light valence quark, and the produced hadrons at large x_F may get quantum numbers that are correlated to those of the valence quark (leading particle effect). The scattering can be from one of the light partons involved in the intrinsic state.

The intrinsic charm production mechanism (Fig. 4(b)) is expected to be smaller than the extrinsic one, due to the $1/m_Q^2$ suppression from the requirement of spatial overlap of initial light partons. However, at sufficiently large x_F the intrinsic mechanism will dominate, because the momentum of several incoming partons can be transferred to the heavy quarks. Our present, improved understanding of intrinsic charm, as outlined above, will allow a more quantitative theoretical discussion of these phenomena than was possible heretofore. Such an analysis will also become increasingly meaningful as the data on hadroproduced charm at large x_F improves.

Experiments on charm production from nuclear targets have shown an anomalous dependence on the nuclear number A . If the open charm (D , Λ_c) cross section is parametrized as

$$\frac{d\sigma}{dx_F} \propto A^{\alpha(x_F)} \quad (7)$$

then $\alpha(x_F \sim 0.2) \sim 0.7 \dots 0.9$ is obtained.^{32,35} For heavy nuclei ($A \approx 200$) this means a factor of $2 \dots 3$ suppression in the cross section, compared to the leading QCD expectation ($\alpha = 1$). In this respect, the charm production data is quite different from that of massive μ -pair production, for which α is found to be very close to 1.³⁶

For J/ψ production, the data on the x_F -dependence of α is particularly detailed,^{37,38} showing a remarkable decrease from $\alpha = 1$ near $x_F = 0$ to $\alpha = 0.7 \dots 0.8$ at large x_F . The data at different beam energies agree, implying that Feynman scaling is valid. It is possible to show that the nuclear suppression is not due solely to the shadowing of the nuclear target structure function.³⁹ The effects of the target structure function can be eliminated by forming cross section ratios at a given value of the fractional momentum (x_2) of the target parton. This does not eliminate the target effects seen in the data, however, implying that the suppression does not factorize into a product of beam and target structure functions, as expected in leading twist. The target dependence thus must be due to a higher twist effect, *i.e.*, one that is of $\mathcal{O}(1/m_Q^2)$, compared to the leading (factorizable) QCD process. This is supported by preliminary data on Υ production,³⁸ which shows a significant but weaker nuclear suppression than for J/ψ production.

At high energies, the $c\bar{c}$ quarks do not have time to separate significantly inside the nucleus. Thus the J/ψ forms only after the charm quarks have left the nuclear environment, and the suppression cannot be related to the size of the J/ψ wave function.¹¹ This is also supported by preliminary data showing that the nuclear suppression for the $\Psi(2S)$ and the J/ψ is the same.³⁸ The $c\bar{c}$ state itself has a finite size, of $\mathcal{O}(1/m_Q^2)$, and could lose some momentum due to rescattering. Due to the rapid decrease of the cross section at large x_F , the trend of this effect is to make α decrease with x_F as observed. However, it is difficult to explain the magnitude of the x_F -dependence of α without assuming the loss of a large fraction of the momentum of the $c\bar{c}$ system.

A natural explanation of the increase of the nuclear suppression in J/ψ production with x_F is provided by the existence of two production mechanisms, the extrinsic and intrinsic ones.⁴⁰ As discussed above, intrinsic charm production is damped by a factor $1/m_c^2$, but can still dominate the small gluon fusion cross section at large x_F . Since the intrinsic heavy quark state tends to have a larger transverse size than the extrinsic one, it will suffer more rescattering in the nucleus. The x_F -dependence of α can then be understood as reflecting the increasing importance of intrinsic Fock states at large x_F . A comprehensive treatment of these effects as well as the suppression of charmonium production at low x_F due to co-moving spectators is given in Ref. 41.

The present experimental evidence for the existence of intrinsic charm in hadronic and nuclear collisions is suggestive but not conclusive. More quantitative studies of

the intrinsic charm wave function, using multiparton distributions, coupled with better data on open charm at large x_F is clearly needed. Electroproduction studies can play a definitive role by measuring the charm structure function in semi-inclusive reactions, and by measuring the distribution of charmed hadrons and charmonium in the large x_F proton fragmentation region.

THE INTRINSIC HARDNESS OF NUCLEAR WAVE FUNCTIONS

We noted above that intrinsic hardness should be enhanced in nuclear wave functions, due to the increased probability for spatial overlap of light partons from different nucleons. All of the data on charm production discussed above was obtained with beams of ordinary hadrons, and the experimental acceptance generally limited the observations to the forward ($x_F > 0$) hemisphere. This data thus reflects the importance of charm in the wave functions of the beam particles. An important exception to this is the EMC measurement of the charm structure function of the Fe nucleus.²¹ An enhancement over the extrinsic photon-gluon contribution was observed at large x_F , but the limited statistics prevented a firm conclusion.

Several features of scattering on nuclear targets show that the nucleus cannot always be treated as a collection of ordinary nucleons. Measurements of deep inelastic lepton scattering have revealed^{42,43,44} deviations of the nuclear structure functions from those of free nucleons, both at very small and at intermediate values of x (the "EMC Effect"). There are also indications⁴⁵ that the quark distributions in nuclei extend beyond $x = 1$. Unusual states of the nucleus could be involved as well in the production of large p_T particles in hadron-nucleus collisions, where the yield is known to increase faster than the nuclear number A (The "Cronin Effect").^{46,47}

The most direct evidence for an enhancement of the nuclear structure function at large x comes from the so-called "Cumulative Effect".⁴⁸ Cumulative particles are defined as hadrons produced in the fragmentation region of a nucleus which have $x_F > 1$, *i.e.*, they carry more momentum than the individual nucleons (apart from Fermi motion effects). In practice, experiments are mostly done by scattering a variety of particles (leptons, hadrons and nuclei) on stationary nuclei, and observing hadrons that are moving backward in the laboratory. A simple kinematical exercise shows that at sufficiently high beam energies, the energy E_h and longitudinal momentum p_h^L of a hadron h produced on a free stationary nucleon must satisfy

$$x \equiv \frac{E_h - p_h^L}{m_N} \leq 1 \quad (8)$$

where m_N is the nucleon mass and $p_h^L < 0$ in the backward direction. The variable x defined by (8) is the usual (light-cone) fractional momentum, which is equivalent to the Feynman momentum fraction x_F of h in the CM system. This equivalence is strictly true for infinite beam momentum; a number of alternative definitions of x have been used in order to take finite energy effects into account. The difference between the various definitions will not be important for our qualitative discussion below.

Cumulative particle production has been seen in many experiments using a variety of beam particles and energies, up to values of $x = 4$ or so. To a first approximation, Feynman scaling (*i.e.*, independence of beam energy) sets in already at quite low energies, $p_{beam} \sim 2 \text{ GeV}$ (Fig. 5(a)). The shape of the cumulative hadron distribution is insensitive to the type of beam particle used. These features suggest that the cumulative particle distribution reflects properties of the nuclear wave function.

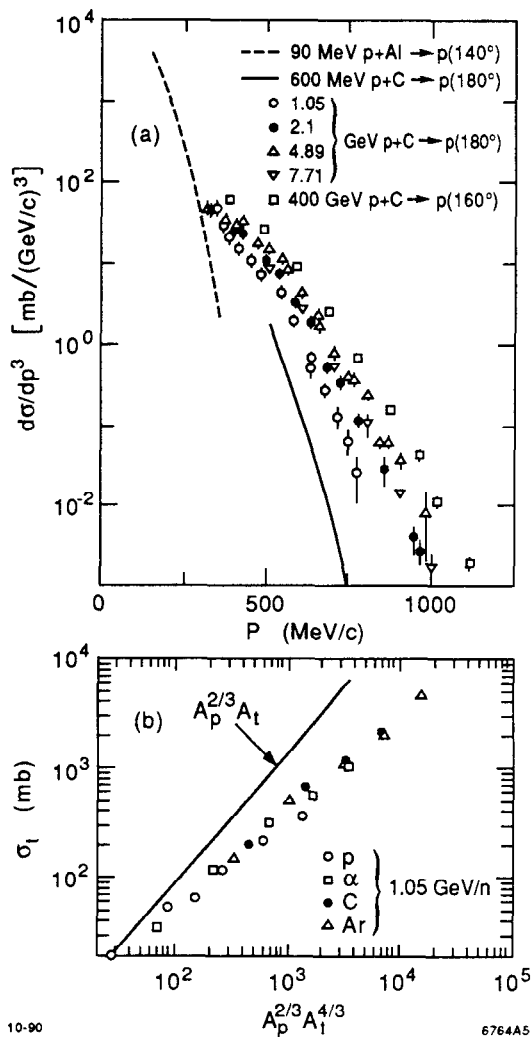


Figure 5. (a) Laboratory momentum distributions of cumulative protons produced by protons scattering on carbon and aluminum nuclei. In an analogy to the Rutherford experiment, the backscattering of 1 GeV protons from a beam of 2 GeV protons suggests encounters with small structures within the nucleus. (b) Dependence on the atomic number of the target (A_t) and projectile (A_p) for cumulative protons in the target fragmentation region. The data were fitted to a gaussian momentum distribution with a total rate parametrized by σ_t , which scales when plotted as a function of $A_p^{2/3} A_t^{4/3}$. Data and further references in Ref. 50.

The laboratory momenta of the cumulative particles range well beyond 1 GeV , making a description in terms of ordinary Fermi motion unlikely. If a nucleon basis is used in the wave function it would be necessary, in this energy range, to include in an essential way also N^* and Y^* excitations. In fact, many arguments⁴⁸ point to the cumulative phenomena being linked to short-distance features of the nuclear wave function. The momenta of several nucleons in a nucleus have to be combined in order to produce the cumulative particles observed at the highest values of x . This presumably requires a close spatial correlation between the nucleons. Such short-distance effects in the nuclear wave function are best described in terms of quark and gluon degrees of freedom.⁴⁹

The dependence of the cumulative particle distribution on the atomic number of the target nucleus is at least as fast as A^1 , and is compatible with $A^{4/3}$ for cumulative protons at lower energies^{50,51} (Fig. 5(b)). An A -dependence this strong suggests that the production of the cumulative partons is a volume effect, with little absorption of the outgoing quanta. An $A^{4/3}$ dependence is what one would naively expect for intrinsic hardness, given that the small size of the hard cluster implies a suppression of rescattering in the nucleus, and taking into account the factor $A^{1/3}$ enhancement from the transverse overlap (of two partons) along the nuclear diameter. For nuclear projectiles, the dependence on the atomic number of the projectile is compatible^{50,51} with $A_{proj}^{2/3}$. For $A_{proj} < A_{target}$, this is also in accord with naive expectations, since the projectile presumably can put intrinsically hard clusters on their mass shell throughout a region of transverse space proportional to the area of the projectile.

Direct evidence that the cumulative phenomenon is associated with small transverse size is provided by the p_T -distribution of the produced hadrons.^{52,53} The average p_T^2 grows rapidly with x , and reaches $2 GeV^2$ for pions at $x = 3$ (Fig. 6(a)). This is expected for the intrinsic configurations (4), since ΔE depends on p_T^2/x (see Eq. (2)). Note that although the individual partons in an intrinsically-hard cluster (*cf.* Fig. 3) have large transverse momenta, the total transverse momentum of the cluster is small. Hence in a case such as J/ψ production, where both intrinsic quarks are incorporated in the same final hadron, much of the large p_T cancels out. On the other hand, when an intrinsic quark combines with a low p_T spectator the final hadron will carry large p_T . The experimental result that cumulative protons tend to have smaller p_T and larger cross section at a given x may be due to more intrinsic partons getting incorporated in the protons than in the pions.⁴⁹

A remarkable feature of the cumulative x -distributions is that their shape is quite similar for all observed particles: protons, positive and negative pions and kaons. Thus, *e.g.*, the ratio between the K^- and π^- yields⁵⁴ shown in Fig. 6(b) is constant over the measured range $1.5 \leq x \leq 2.5$. This differs from the fragmentation of single nucleons,⁵⁵ for which this ratio decreases as $x \rightarrow 1$. The magnitude of the K^+ yield is⁵⁴ also much higher than would be naively expected. The heaviest nuclear targets produce roughly equal numbers of K^+ and π^+ mesons at $x \geq 1.5$.

For intrinsically-hard quarks we have noted that the x -distribution should be similar

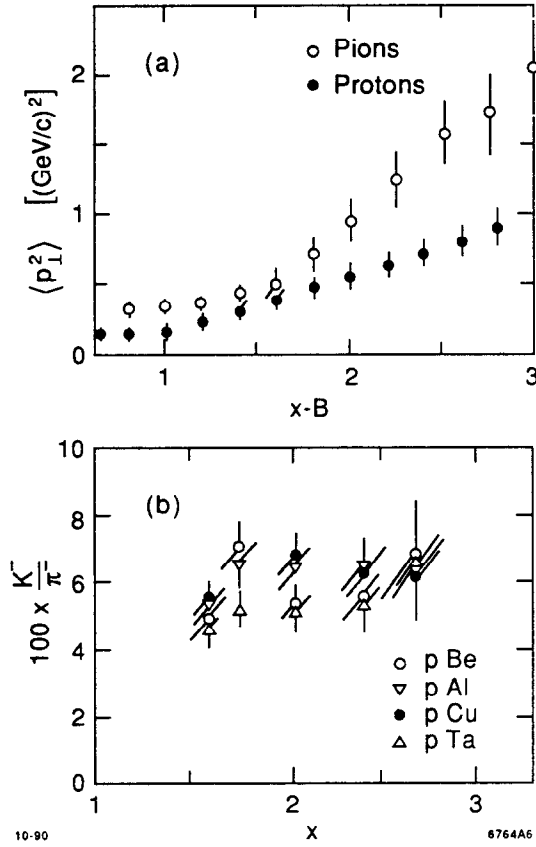


Figure 6. (a) The mean square transverse momentum of cumulative pions (\circ) and protons (\bullet) produced by 10 GeV protons on Ta and Pb. The scale of the x -axis is offset by $B = 1$ for the protons ($B = 0$ for the pions). Data from Ref. 52. (b) The ratio of cumulative K^- to π^- production on several nuclei as a function of x . Data from Ref. 54.

for all quarks in a given range of p_T or quark mass, according to Eqs. (5) and (6). At the x -values considered here, the typical p_T -values are larger than, or at least comparable to, the strange quark mass (*cf.* Fig. 6(a)). Hence the π and K mesons produced by intrinsic u , d and s quarks are expected to have similar x -distributions, as observed. The K^+ mesons can get their momenta from intrinsic u valence quarks. Since the creation of an $s\bar{s}$ pair is not suppressed at the relatively large p_T -scale involved, we can understand the equality of the K^+ and π^+ meson rates. The production of a K^- meson at large x , on the other hand, requires an energetic \bar{u} or s sea quark. In this case momentum must be transferred from the valence quarks and gluons according to Fig. 2. Hence it is not surprising that the rate of K^- -mesons is suppressed by about a factor 20 in the cumulative region, as seen in Fig. 6(b).

Our interpretation of the cumulative phenomena in terms of an enhancement in the nuclear structure function for $x > 1$ is compatible with some earlier suggestions.^{47,48,56,57} Models of multiquark bags have been used to provide a unified explanation of the EMC, Cronin, and Cumulative Effects. An analysis of the EMC Effect in fact suggested the

existence of a small admixture in nuclear wave functions of "collective" sea quarks, which are as energetic as the valence quarks.⁵⁸ The multiquark bag models do not, however, predict the probability for bag formation, nor the x -distributions of the quarks in the bag. The properties of the intrinsically-hard component of nuclear wave functions, on the other hand, can be calculated from perturbative QCD in terms of the known quark and gluon distribution functions of nucleons. An immediate consequence is that the multiquark correlations must have a small transverse range, implying an increase of the average p_T at large x , as observed in the data (Fig. 6(a)).

Other puzzles involving fast nuclear fragments, which also may be related to intrinsic hardness, include the production of particles from nuclei below threshold for collisions on free nucleons. For example, subthreshold production of antiprotons has been observed both in $p + Cu$ and $Si + Si$ collisions.⁵⁹ While the \bar{p} rate was thought to be understood for the $p + Cu$ data, based on the high cumulative momenta being interpreted as due to Fermi motion, it turned out that the corresponding calculation underestimated the rate for $Si + Si$ collisions by three orders of magnitude. In our view, the cumulative momenta should be discussed at the parton level. The rate for \bar{p} production may then proceed much more favorably through, *e.g.*, the $gg \rightarrow p\bar{p}$ reaction, whose threshold is just $2m_p$ in the center-of-mass.

Clearly the most unambiguous way to unravel the mysteries of cumulative effects and other high momentum nuclear enhancements is to study the nuclear target fragmentation region in electroproduction $eA \rightarrow e'HX$ both at large negative x_F and in the subthreshold region since the basic interaction of the photon probe with the quark currents of the nucleus is well-understood.

ACKNOWLEDGEMENTS

Some of the material presented above is based on collaborations with G. de Teramond and I. Schmidt. PH wishes to thank the SLAC theory group for its warm hospitality during his sabbatical. Part of this talk was also presented at the Topical Conference on Particle Production near Threshold, Nashville, Indiana, 1990.

REFERENCES

1. For a review of QCD physics at HERA see S. J. Brodsky, SLAC-PUB 5312 and 5313 (1990.)
2. S. J. Brodsky, J. R. Cudell, and P. V. Landshoff, in preparation.
3. S. J. Brodsky, P. Hoyer, and A. H. Mueller, in preparation.
4. See S. J. Brodsky and G. P. Lepage, in *Quantum Chromodynamics*, edited by A. H. Mueller, (World Scientific, 1990 and references therein.)
5. S. J. Brodsky, SLAC-PUB-5382 (1990), SLAC-PUB 5371 (1990), and SLAC-PUB-5013, published in the *Proceedings of the Topical Conf. on Electronuclear Physics with Internal Targets*, Stanford, CA, Jan 9-12, 1989.

6. For a quantum mechanical derivation in gauge theory and references to earlier work see G. Bodwin, S. J. Brodsky, and G. P. Lepage, Phys. Rev. D39, 3287 (1989).
7. S. J. Brodsky and H. J. Lu, Phys. Rev. Lett. 64, 1342 (1990).
8. E. L. Berger and S. J. Brodsky, Phys. Rev. Lett. 42, 940 (1979).
9. J.-w. Qiu and G. Sterman, Stony Brook preprint ITP-SB-90-45, (1990).
10. R.L. Jaffe and A. Manohar, Nucl. Phys. B321, 343 (1989).
11. A. H. Mueller, *Proc. XVII Recontre de Moriond* (1982); S. J. Brodsky, *Proc. XIII International Symposium on Multiparticle Dynamics*, Volendam (1982); S. J. Brodsky and A. H. Mueller, Phys. Lett. 206B, 685 (1988), and references therein.
12. J. P. Ralston and B. Pire, Phys. Rev. Lett. 61, 1823 (1988), University of Kansas preprint 90-0548 (1990); and this conference.
13. B. K. Jennings and G. A. Miller, Phys. Lett. B236, 209 (1990). and University of Washington preprint 40427-20-N90 (1990).
14. G. R. Farrar, H. Liu, L. L. Frankfurt, M. I. Strikman, Phys. Rev. Lett. 61, 686 (1988).
15. G. Bertsch, S. J. Brodsky, A. S. Goldhaber, and J. Gunion, Phys. Rev. Lett. 47, 297 (1981).
16. A. S. Carroll, *et al.*, Phys. Rev. Lett. 61, 1698 (1988).
17. G. R. Court, *et al.*, Phys. Rev. Lett. 57, 507 (1986).
18. S. J. Brodsky and G. de Teramond, Phys. Rev. Lett. 60, 1924 (1988).
19. S. J. Brodsky, G. de Teramond, and I. Schmidt, Phys. Rev. Lett. 64, 1011 (1990).
20. The signal for the production of almost-bound nucleon (or nuclear) charmonium systems near threshold is the isotropic production of the recoil nucleon (or nucleus) at large invariant mass $M_X \simeq M_{\eta_c}$.
21. J. J. Aubert, *et al.*, Nucl. Phys. B213, 31 (1983). See also E. Hoffmann and R. Moore, Z. Phys. C20, 71 (1983).
22. G. P. Lepage, S. J. Brodsky, T. Huang, and P. Mackenzie, published in the proc. of the *Banff Summer Institute* (1981).
23. K. Hornbostel, S. J. Brodsky, and H. C. Pauli, Phys. Rev. D41, 3814 (1990), and references therein.
24. S. J. Brodsky and I. A. Schmidt, Phys. Rev. D43, 179 (1991).
25. S. J. Brodsky, P. Hoyer, C. Peterson, and N. Sakai, Phys. Lett. 93B, 451 (1980); S. J. Brodsky, C. Peterson, and N. Sakai, Phys. Rev. D23, 2745 (1981).
26. S. J. Brodsky, H. E. Haber, and J. F. Gunion, in *Anti-pp Options for the Supercollider*, Division of Particles and Fields Workshop, Chicago, IL, 1984, edited by J. E. Pilcher and A. R. White (SSC-ANL Report No. 84/01/13, Argonne, IL, 1984), p. 100; S. J. Brodsky, J. C. Collins, S. D. Ellis, J. F. Gunion, and A. H. Mueller, published in Snowmass Summer Study 1984, p. 227.
27. C. Peterson, D. Schlatter, I. Schmitt and P. M. Zerwas, Phys. Rev. D27, 105 (1983).

28. R. J. Cashmore, *Proc. Int. Symp. on Prod. and Decay of Heavy Flavours*, Stanford 1987 (E. Bloom and A. Fridman, Eds.), p.118.
29. L. V. Gribov, E. M. Levin and M. G. Ryskin, *Nucl. Phys.* **B188**, 555 (1981) and *Phys. Rep.* **100**, 1 (1983); A. H. Mueller and J. Qiu, *Nucl. Phys.* **B268**, 427 (1986).
30. F. E. Close, J. Qiu and R. G. Roberts, *Phys. Rev.* **D40**, 2820 (1989).
31. A. Kernan and G. VanDalen, *Phys. Rep.* **106**, 297 (1984), and references therein.
32. S. P. K. Tavernier, *Rep. Prog. Phys.* **50**, 1439 (1987); U. Gasparini, *Proc. XXIV Int. Conf. on High Energy Physics*, (R. Kotthaus and J. H. Kühn, Eds., Springer 1989), p. 971.
33. S. F. Biagi, *et al.*, *Z. Phys.* **C28**, 175 (1985); P. Chauvat, *et al.*, *Phys. Lett.* **199B**, 304 (1987); P. Coteus, *et al.*, *Phys. Rev. Lett.* **59**, 1530 (1987); C. Shipbaugh, *et al.*, *Phys. Rev. Lett.* **60**, 2117 (1988); M. Aguilar-Benitez, *et al.*, *Z. Phys.* **C40**, 321 (1988).
34. M. Aguilar-Benitez, *et al.*, *Phys. Lett.* **161B**, 400 (1985) and *Z. Phys.* **C31**, 491 (1986); S. Barlag, *et al.*, *Z. Phys.* **C39**, 451 (1988) and CERN-PPE/90-145 (1990).
35. M. MacDermott and S. Reucroft, *Phys. Lett.* **184B**, 108 (1987); H. Cobbaert, *et al.*, *Phys. Lett.* **191B**, 456 (1987), *ibid.*, **206B**, 546 (1988) and *Z. Phys.* **C36**, 577 (1987); M. E. Duffy, *et al.*, *Phys. Rev. Lett.* **55**, 1816 (1985); M. I. Adamovich, *et al.*, CERN-EP/89-123 (1989).
36. K. J. Anderson, *et al.*, *Phys. Rev. Lett.* **42**, 944 (1979); A. S. Ito, *et al.*, *Phys. Rev.* **D23**, 604 (1981); J. Badier, *et al.*, *Phys. Lett.* **104B**, 335 (1981); P. Bordalo, *et al.*, *Phys. Lett.* **193B**, 368 (1987).
37. Yu. M. Antipov, *et al.*, *Phys. Lett.* **76B**, 235 (1978); M. J. Corden, *et al.*, *Phys. Lett.* **110B**, 415 (1982); J. Badier, *et al.*, *Z. Phys.* **C20**, 101 (1983); S. Katsanevas, *et al.*, *Phys. Rev. Lett.* **60**, 2121 (1988).
38. D. M. Alde, *et al.*, *Phys. Rev. Lett.* **64**, 2479 (1990) and Los Alamos preprint LA-UR-90-2331 (1990); C. S. Mishra, *et al.*, Contribution to the XXVth Rencontres de Moriond, Les Arcs (1990), Fermilab-Conf-90/100-E (May 1990).
39. P. Hoyer, M. Vanttinen and U. Sukhatme, *Phys. Lett.* **246B**, 217 (1990).
40. S. J. Brodsky and P. Hoyer, *Phys. Rev. Lett.* **63**, 1566 (1989).
41. R. Vogt, S. J. Brodsky, and P. Hoyer, SLAC-PUB 5421 (1991).
42. J. J. Aubert, *et al.*, *Phys. Lett.* **123B**, 275 (1983); J. Ashman *et al.*, *Phys. Lett.* **202B**, 603 (1988); M. Arneodo *et al.*, *Phys. Lett.* **211B**, 493 (1988).
43. R. G. Arnold *et al.*, *Phys. Rev. Lett.* **52**, 727 (1984).
44. G. Bari, *et al.*, *Phys. Lett.* **163B**, 282 (1985).
45. I. Savin, *Proc. XXII Conf. on High Energy Physics*, Leipzig 1984 (A. Meyer and E. Wieczorek, Eds.) Vol II, p. 251; W. P. Schütz, *et al.*, *Phys. Rev. Lett.* **38**, 259 (1977).
46. J. W. Cronin, *et al.*, *Phys. Rev.* **D11**, 3105 (1975); C. Bromberg, *et al.*, *Phys. Rev. Lett.* **42**, 1202 (1979).

47. A. V. Efremov, V. T. Kim and G. I. Lysakov, *Sov. J. Nucl. Phys.* **44**, 151 (1986); S. Gupta and R. M. Godbole, *Phys. Rev.* **D33**, 3453 (1986), *Z. Phys.* **C31**, 475 (1986) and *Phys. Lett.* **228B**, 129 (1989).
48. For experimental and theoretical reviews of the cumulative effect, see: V. S. Stavinskii, *Sov. J. Part. Nucl.* **10**, 373 (1979); V. B. Gavrilov and G. A. Laksin, preprint ITEP 128-89 (1989); A. V. Efremov, *Sov. J. Part. Nucl. Phys.* **13**, 254 (1982); L. L. Frankfurt and M. I. Strikman, *Phys. Rep.* **76**, 215 (1981) and *Phys. Rep.* **160**, 235 (1988).
49. The fact that the number of cumulative nucleons is much larger than the number of cumulative pions (see Ref. 48) does, however, imply that the recombination of several quarks must be taken into account when using the parton basis to describe cumulative nucleons.
50. J. V. Geagea, *et al.*, *Phys. Rev. Lett.* **45**, 1993 (1980).
51. All the available data cannot, however, be fitted with a simple A^α power law dependence. See also: Yu. D. Bayukov, *et al.*, *Phys. Rev.* **C20**, 764 (1979) and *Sov. J. Nucl. Phys.* **42**, 238 (1985); S. Frankel, *et al.*, *Phys. Rev.* **C20**, 2257 (1979); N. A. Nikiforov, *et al.*, *Phys. Rev.* **C22**, 700 (1980); M. Kh. Anikina, *et al.*, *Sov. J. Nucl. Phys.* **40**, 311 (1984); G. R. Gulkanyan, *et al.*, *Sov. J. Nucl. Phys.* **50**, 259 (1989).
52. S. V. Boyarinov, *et al.*, *Sov. J. Nucl. Phys.* **46**, 871 (1987).
53. A. I. Anoshin, *et al.*, *Sov. J. Nucl. Phys.* **36**, 400 (1982); K. Eqiyan, *Sov. J. Nucl. Phys.* **37**, 731 (1983); , A. M. Baldin, *et al.*, *Sov. J. Nucl. Phys.* **39**, 766 (1984).
54. S. V. Boyarinov, *et al.*, *Sov. J. Nucl. Phys.* **50**, 996 (1989).
55. P. Capiluppi, *et al.*, *Nucl. Phys.* **B79**, 189 (1974).
56. A. M. Baldin, *Nucl. Phys.* **A434**, 695 (1985).
57. A. V. Efremov, *Sov. J. Nucl. Phys.* **24**, 633 (1976); G. Berlad, A. Dar and G. Eilam, *Phys. Lett.* **93B**, 86 (1980); C. E. Carlson, K. E. Lassila and U. P. Sukhatme, preprint WM-90-115 (1990).
58. A. V. Efremov, *Phys. Lett.* **174B**, 219 (1986); A. V. Efremov, A. B. Kaidalov, V. T. Kim, G. I. Lykasov and N. V. Slavin, *Sov. J. Nucl. Phys.* **47**, 868 (1988).
59. J. B. Carroll, *et al.*, *Phys. Rev. Lett.* **62**, 1829 (1989); A. Shor, *et al.*, *Phys. Rev. Lett.* **63**, 2192 (1989), and references therein.